SIM Translation Table

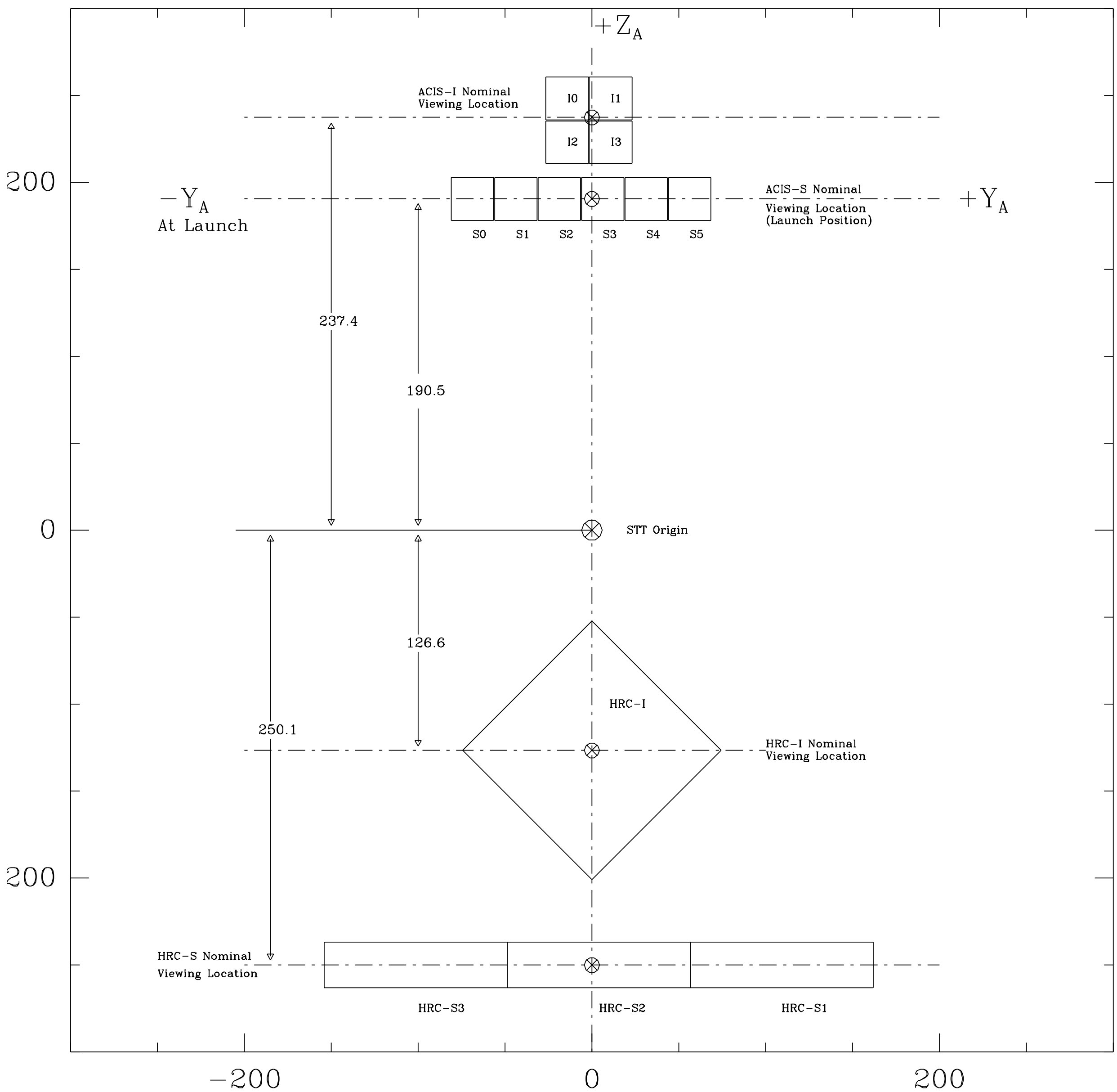

Figure 1: The Chandra SIM Translation Table, showing the flight focal plane instrument to scale. Distance in mm. Coordinate system is AXAF-STT-1.0. (credit: Jonathan McDowell)

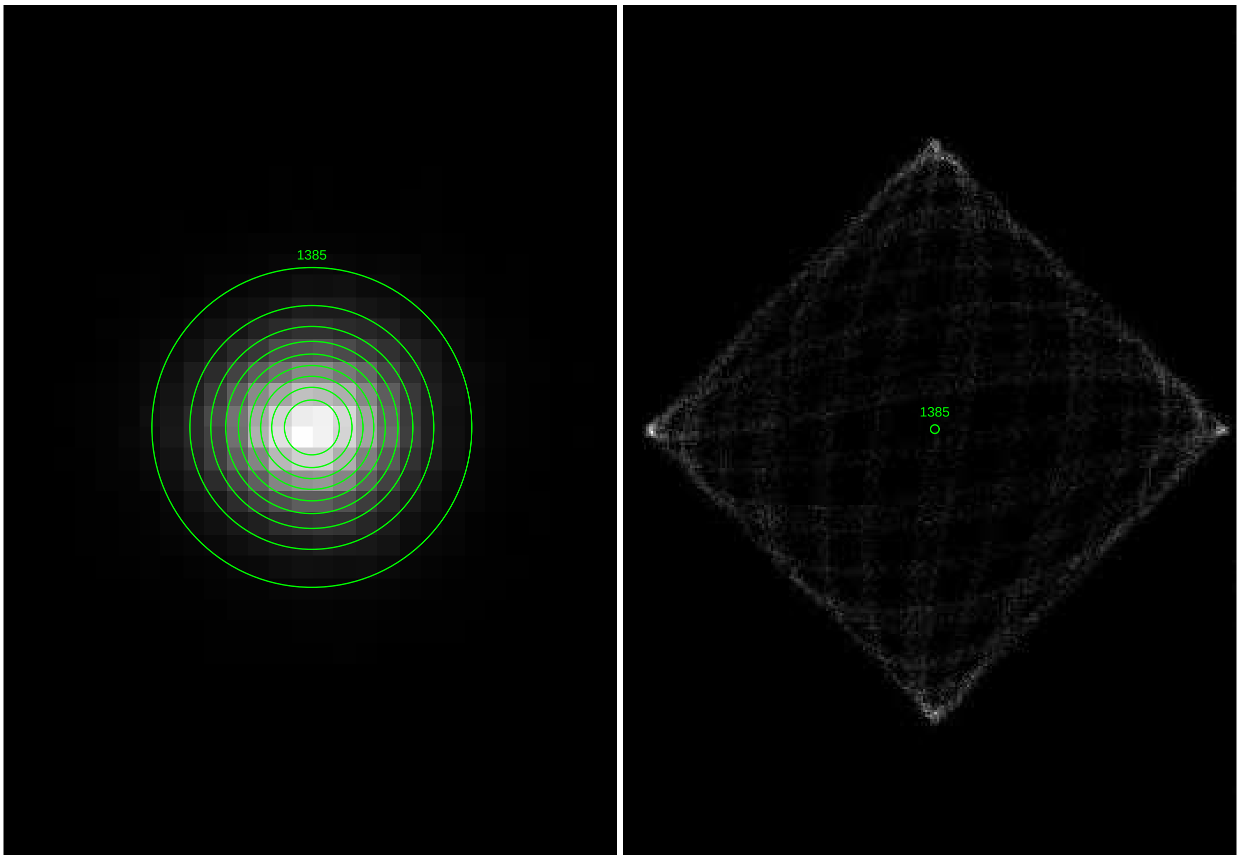

Figure 2: HRC-I observation of Ar Lac with 19ks exposure time and zero Y and Z offsets (obsid 1385). Left: image in sky coordinates with 10% – 90% encircled energy circle overlay. Right: image in chip coordinates with the centriod of the dither pattern marked. The centroid is at the center of the Lissajous dither pattern.

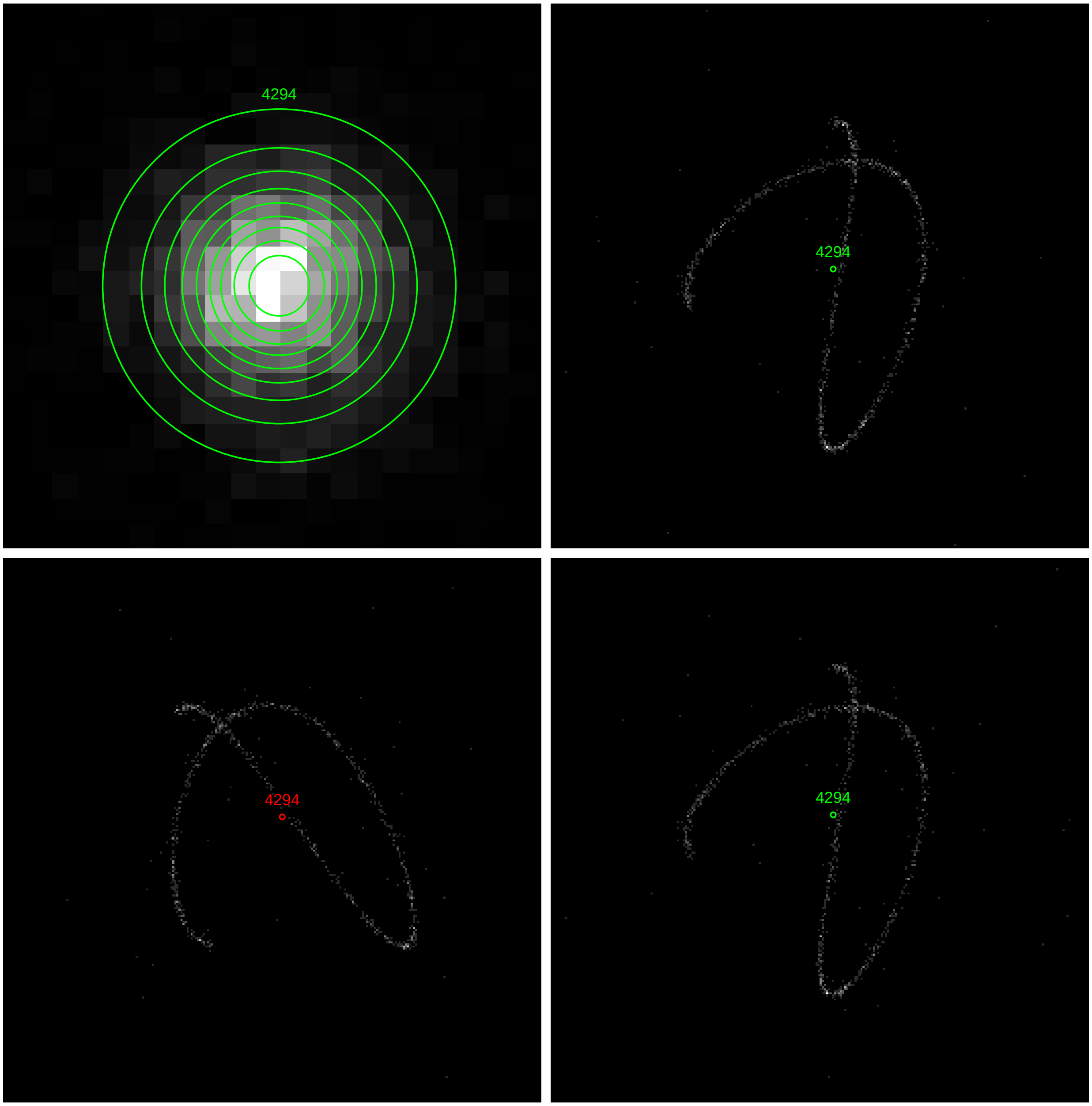

Figure 3: HRC-I observation of Ar Lac with 1ks exposure time and zero Y and Z offsets (obsid 4294). UL: image in sky coordinates with 10% – 90% encircled energy circle overlay; UR: image in chip coordinates with the centriod of the dither pattern marked; LL: image in det coordinates with the centriod of the dither pattern marked; LR: image in tdet coordinates with the centriod of the dither pattern marked.

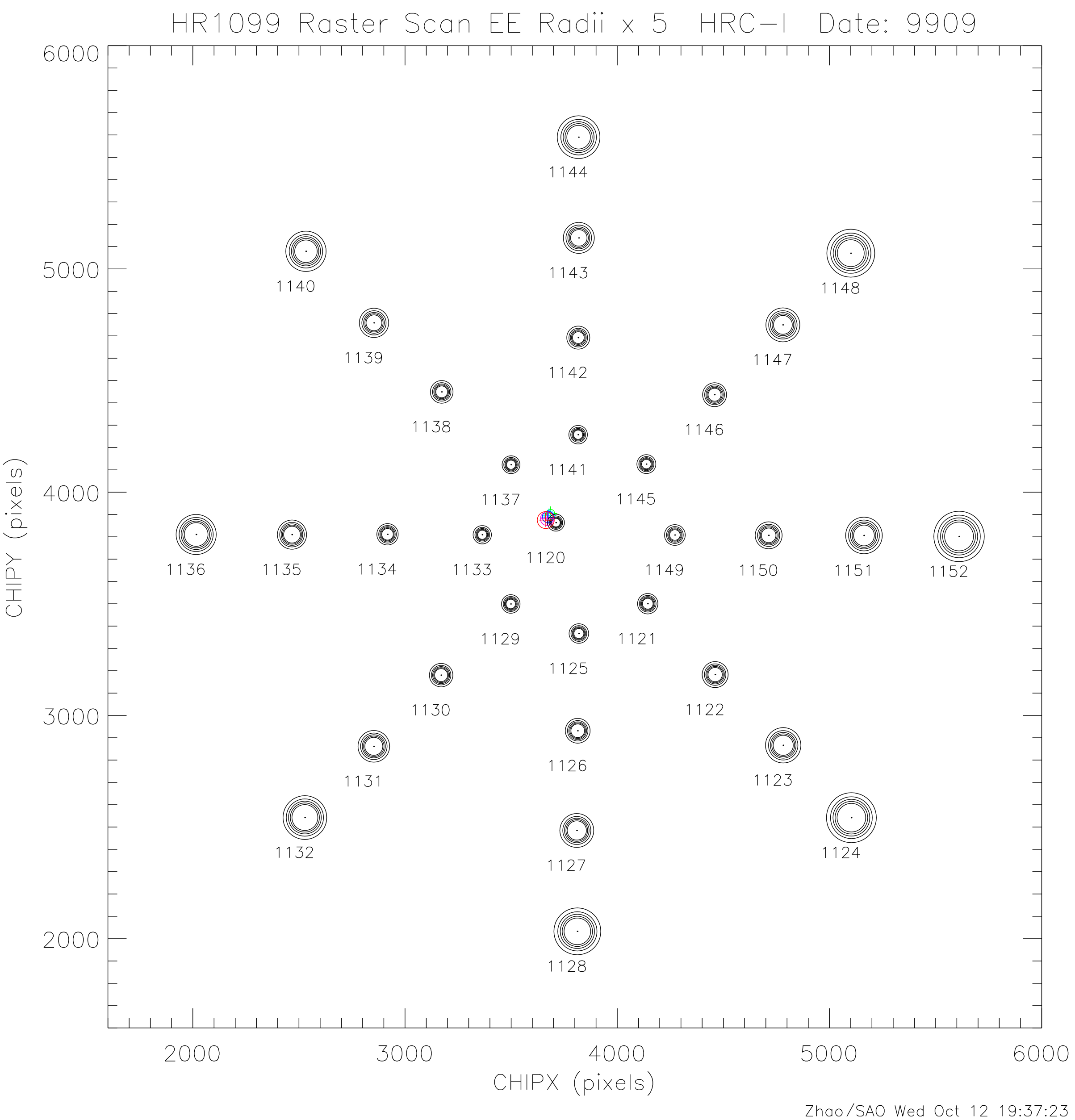

Figure 4: HRC-I raster scan observation of HR 1099 with 1ks exposure time for each scan point (Date: 1999-09-02). Circles around each observation point are the 50% – 90% EE circles × 5.

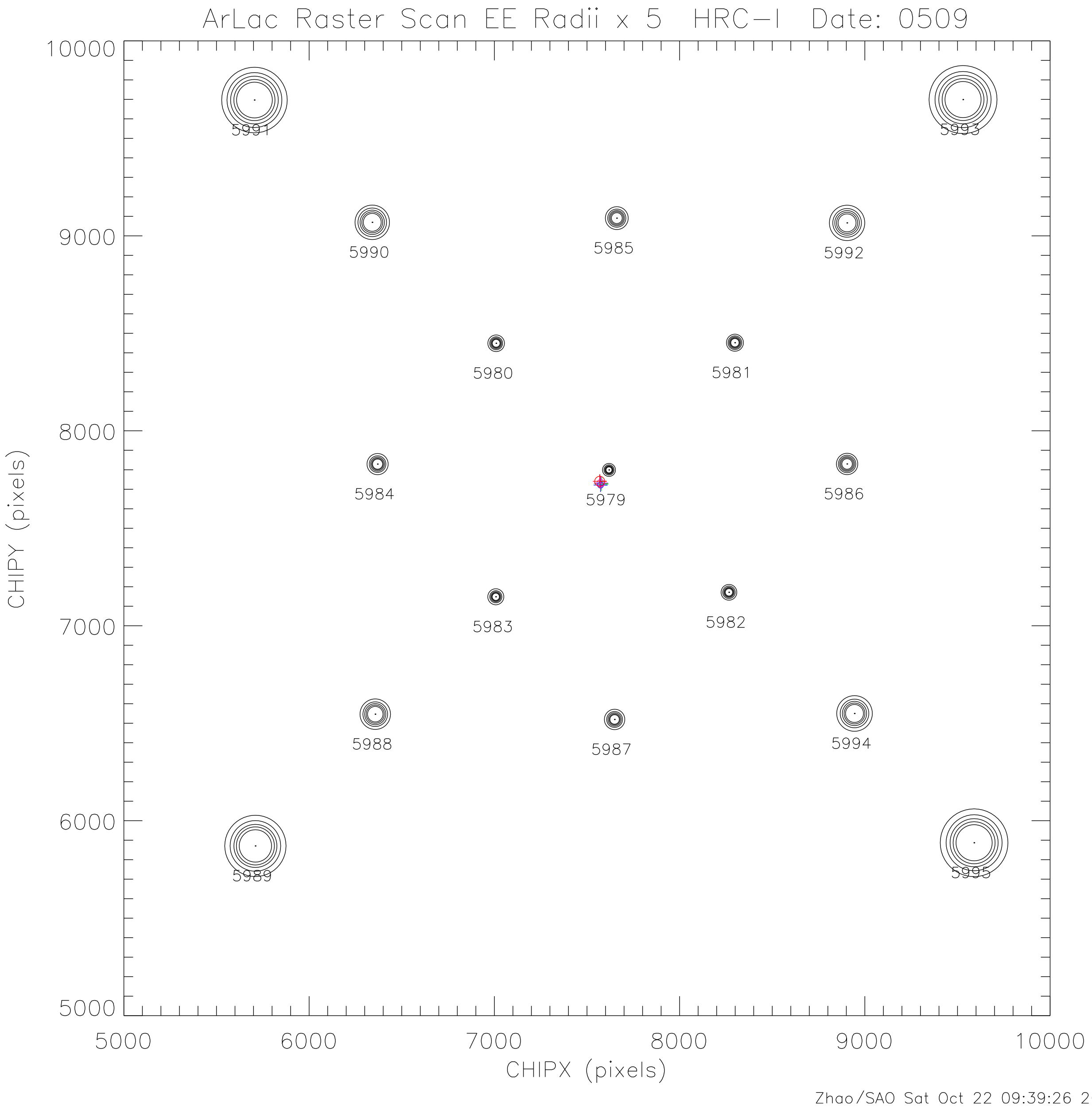

Figure 5: HRC-I raster scan observation of Ar Lac with 1ks exposure time for each scan point (Date: 2005-09-27). Circles around each observation point are the 50% – 90% EE circles × 5.

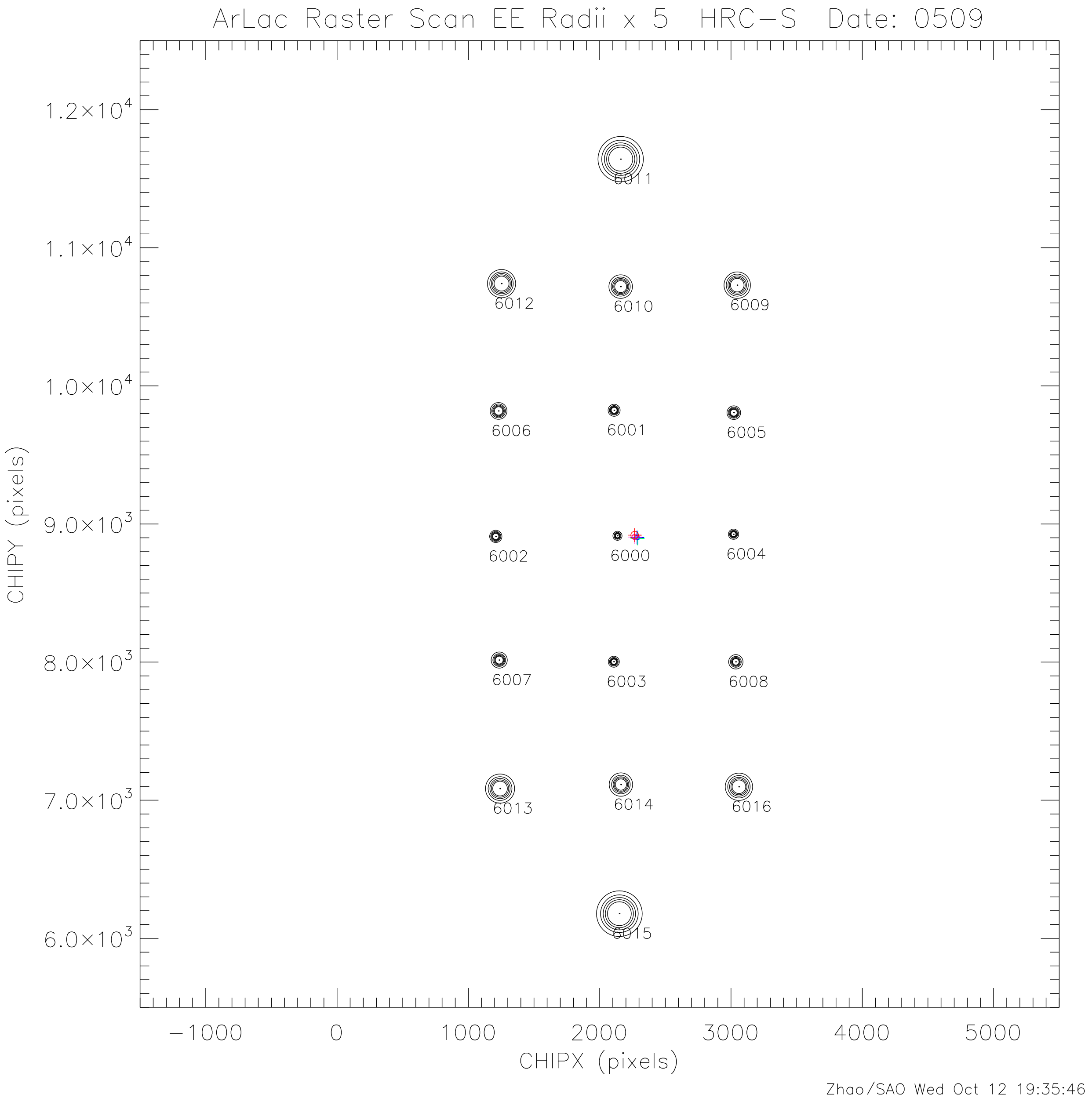

Figure 6: HRC-S raster scan observation of Ar Lac with 1ks exposure time for each scan point (Date: 2005-09-01). Circles around each observation point are the 50% – 90% EE circles × 5.

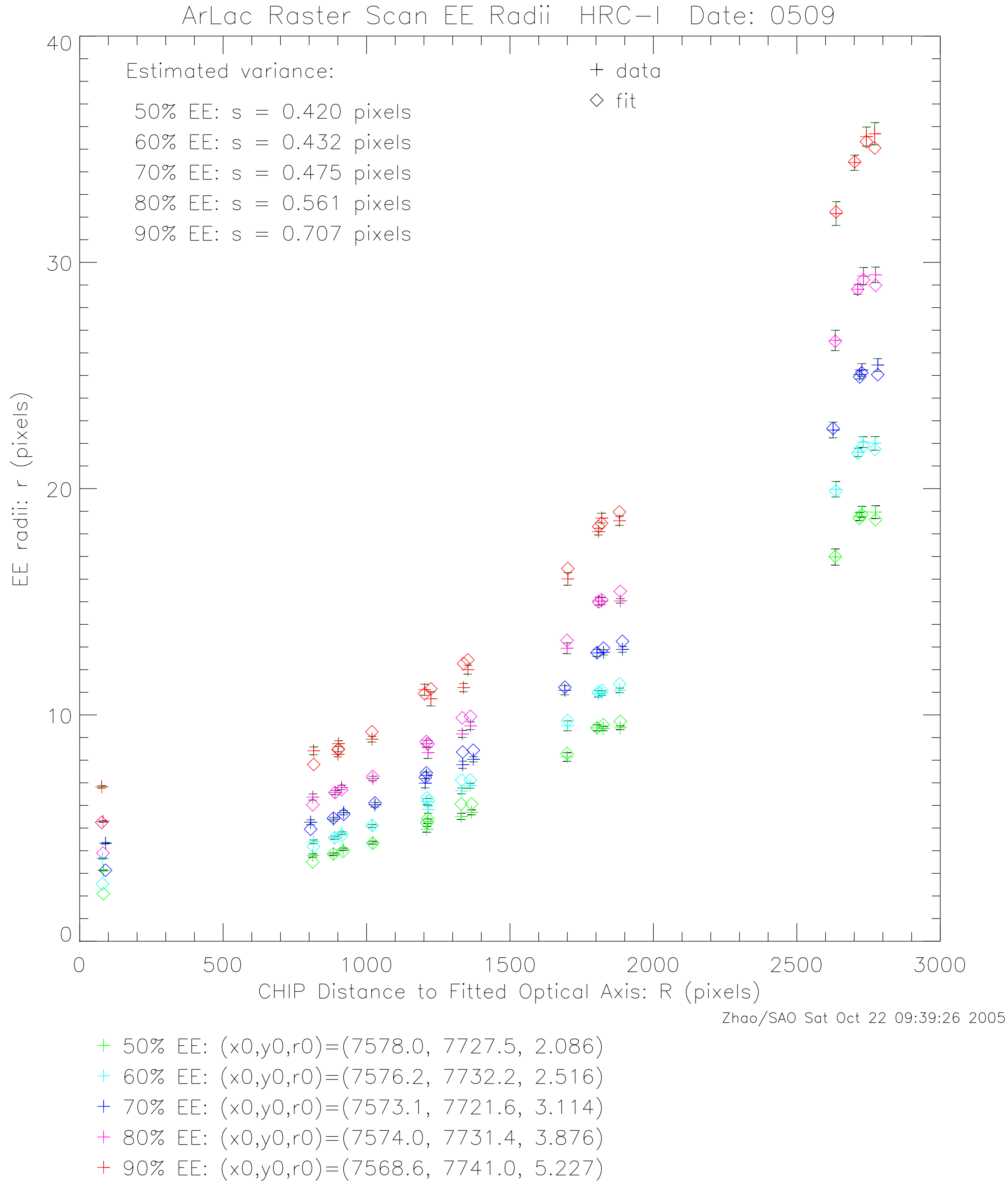

Figure 7: Quadratic fit of HRC-I raster scan data of Ar Lac (Date: 2005-09-27).

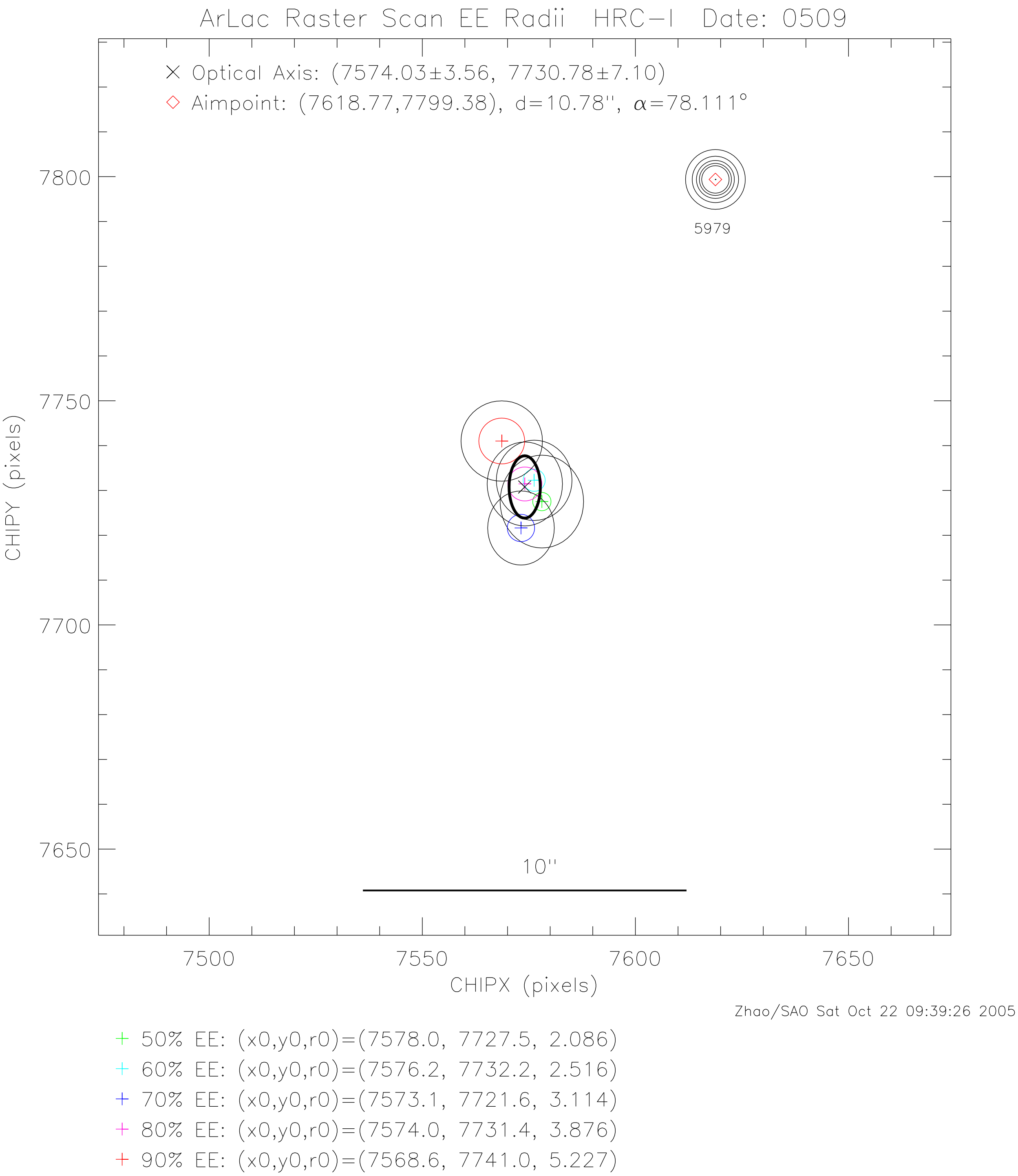

Figure 8: Optical Axis and Aimpoint position on HRC-I, based on raster scan observation of Ar Lac made on 2005-09-27.

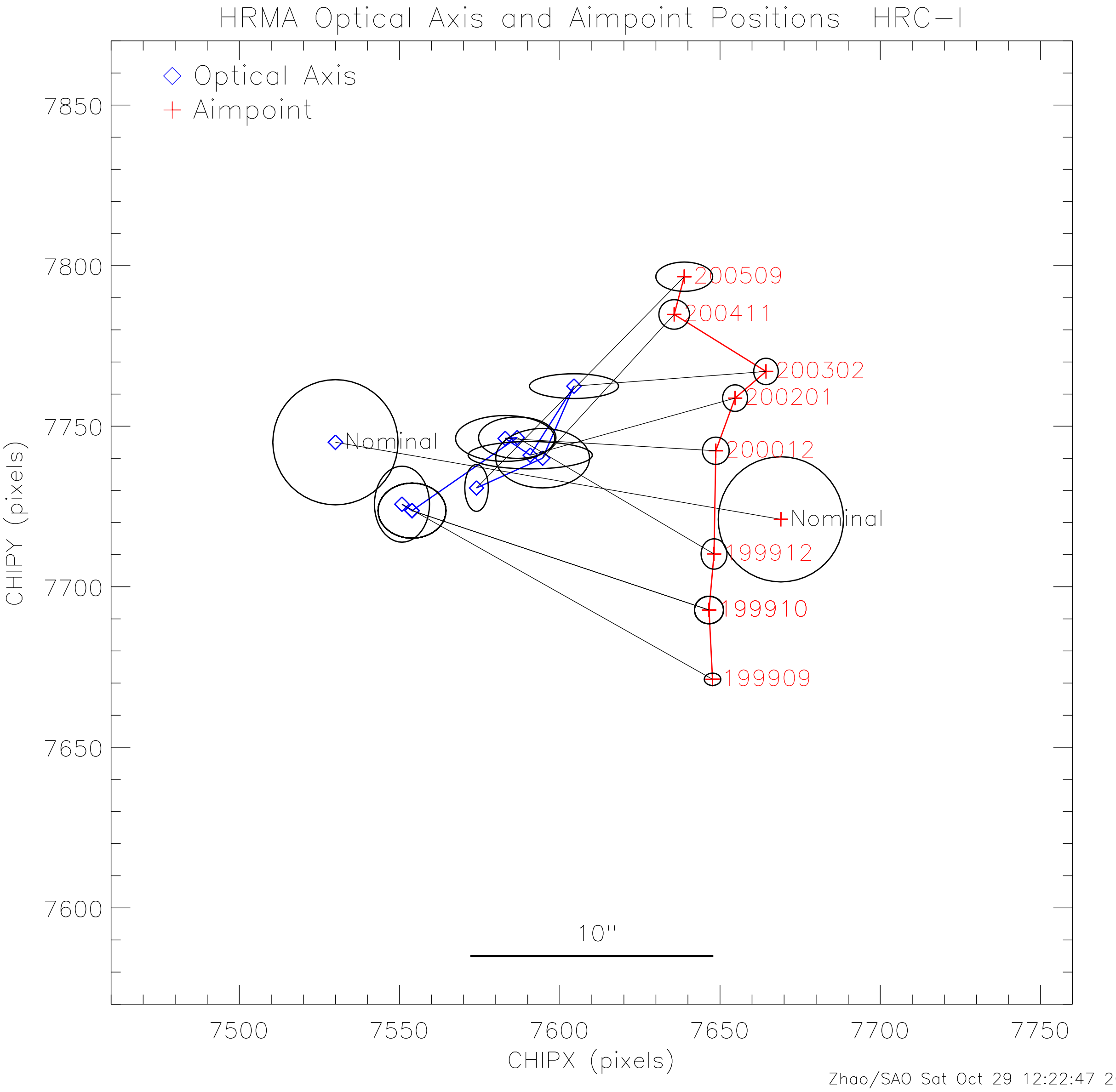

Figure 9: Optical Axis and Aimpoint positions from all the HRC-I measurements on CHIP coordinates.

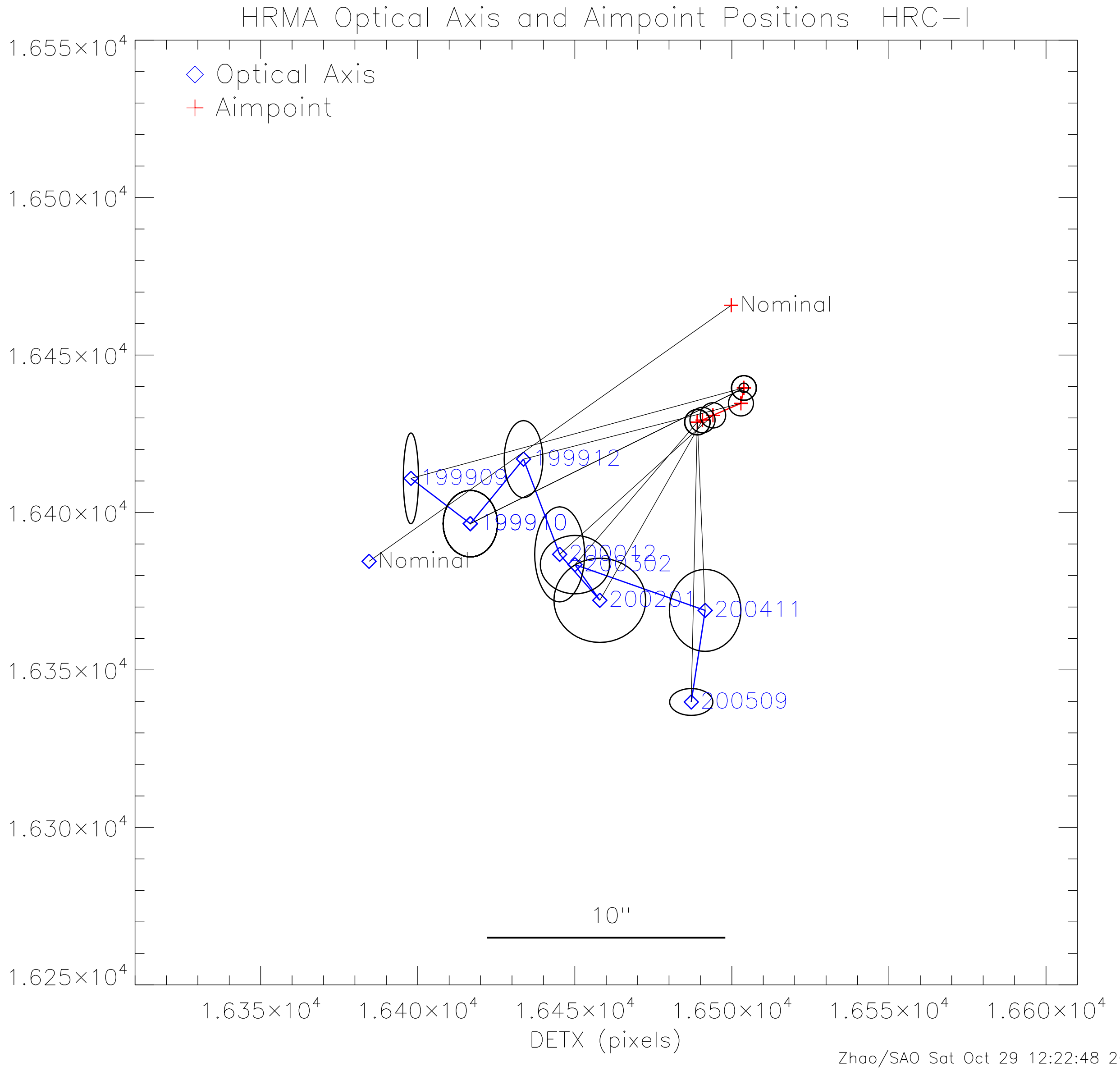

Figure 10: Optical Axis and Aimpoint positions from all the HRC-I measurements on DET coordinates.

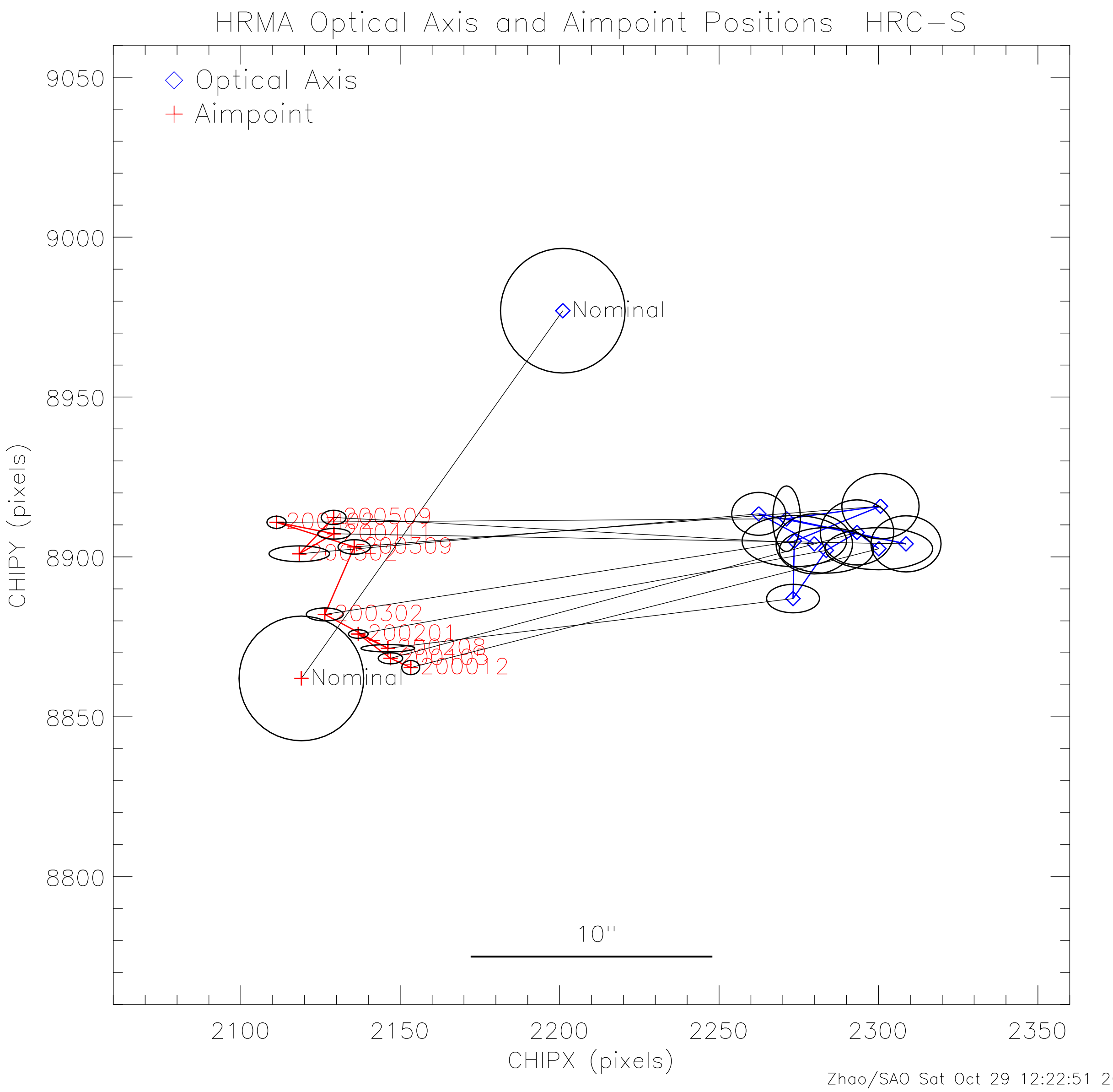

Figure 11: Optical Axis and Aimpoint positions from all the HRC-S measurements on CHIP coordinates.

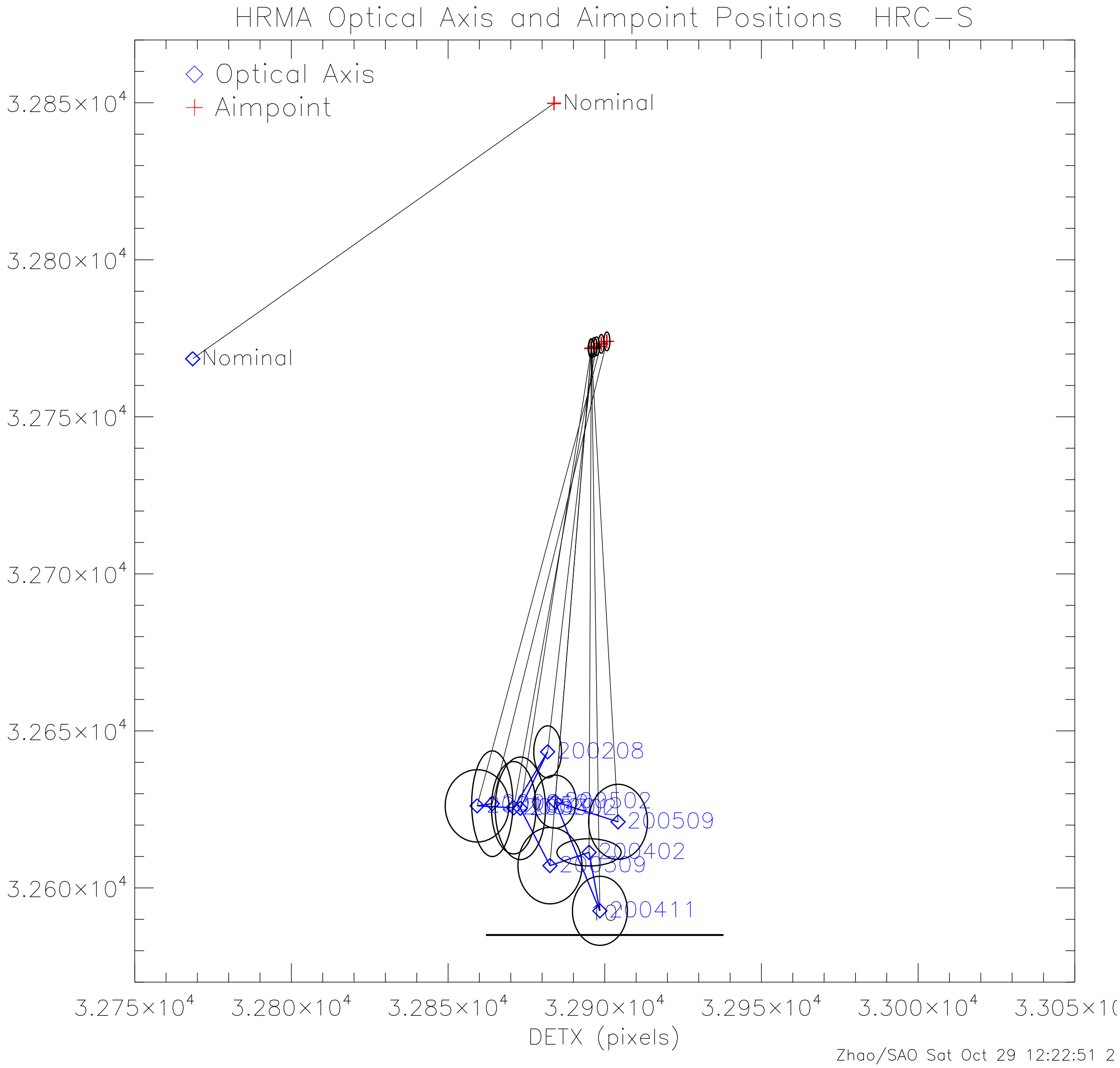

Figure 12: Optical Axis and Aimpoint positions from all the HRC-S measurements on DET coordinates.

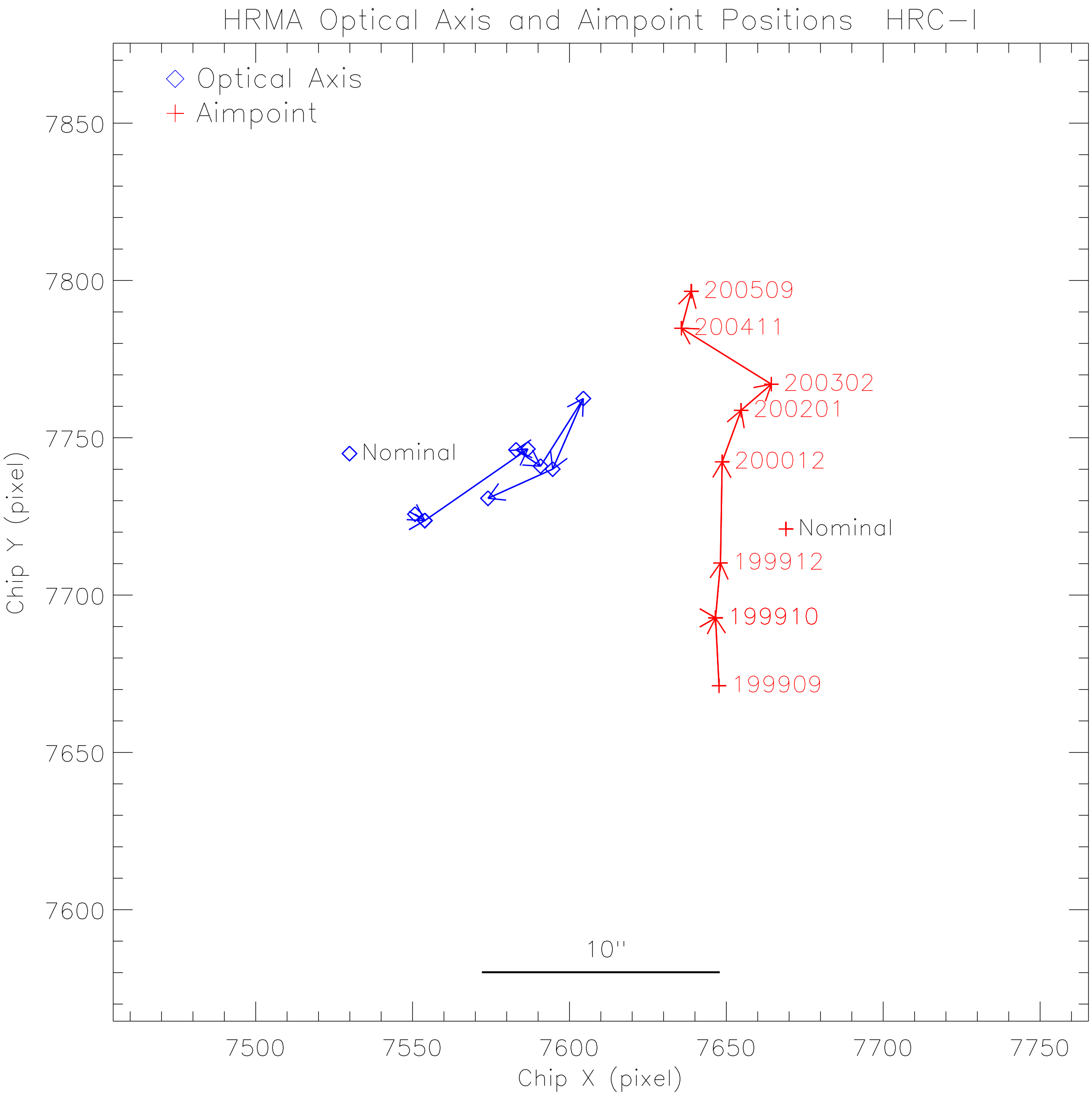

Figure 13: Chandra Optical Axis and Aimpoint positions on HRC-I.

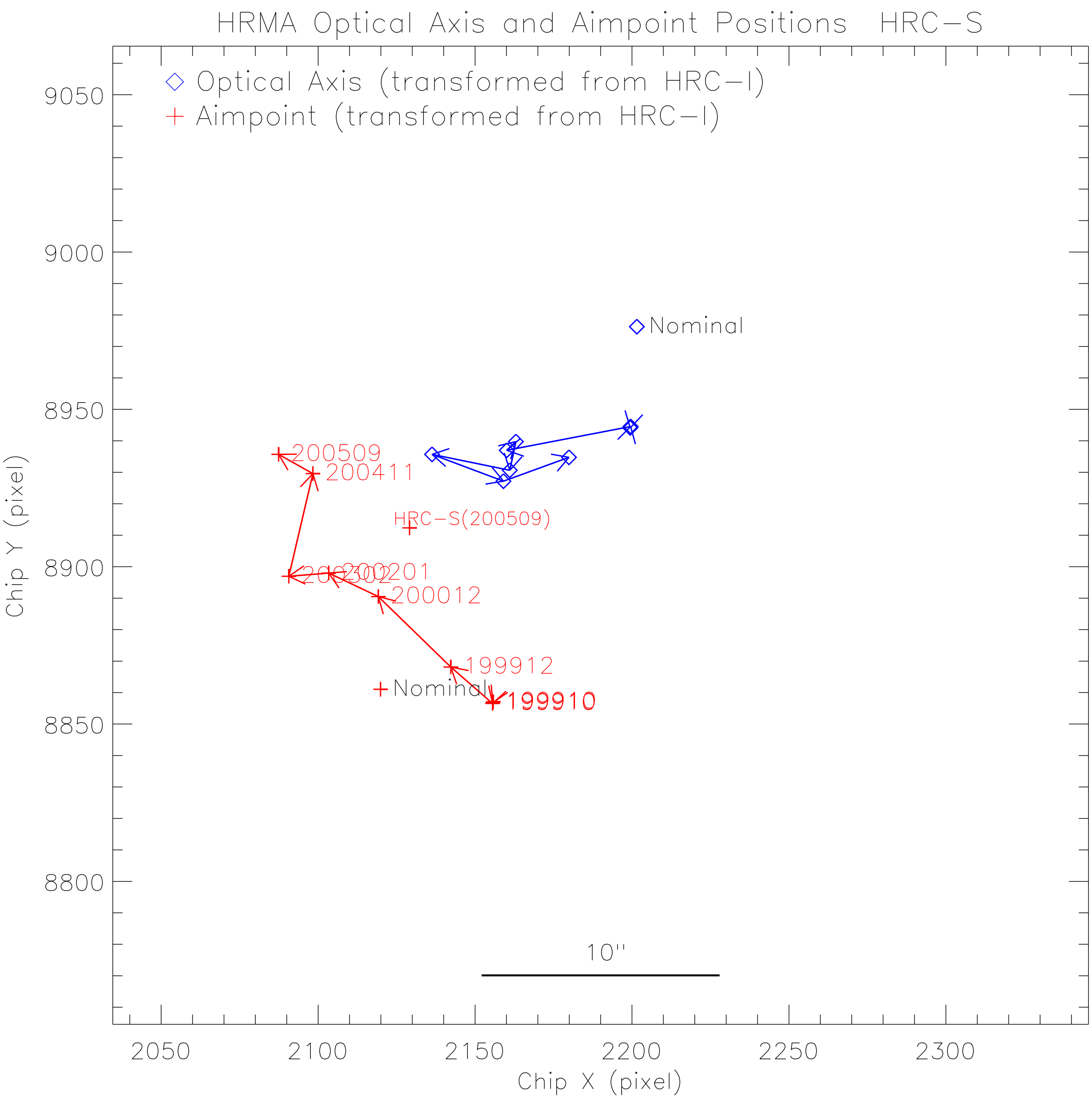

Figure 14: Chandra Optical Axis and Aimpoint positions on HRC-S, transformed from the HRC-I measurements.

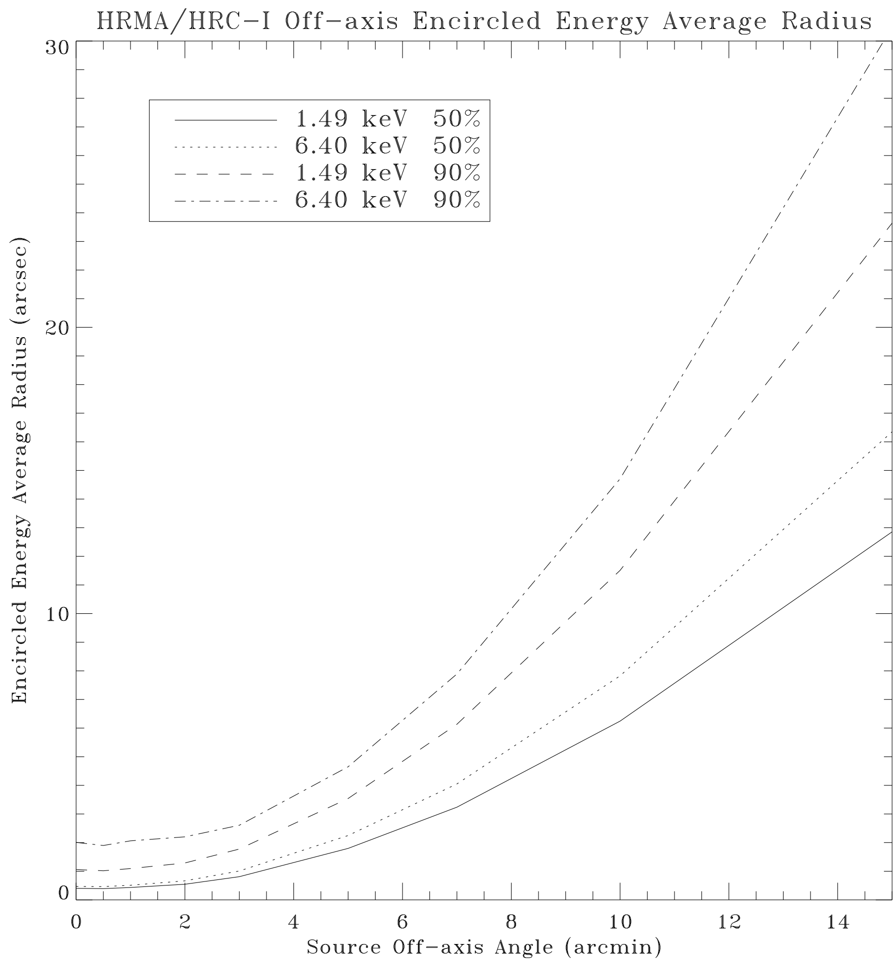

Figure 4.11: **HRMA**/HRC-I encircled energy average radii for circles enclosing 50% and 90% of the power at 1.49 and 6.40 keV as a function of off-axis angle. The HRC-I surface is a flat plane perpendicular to the optical axis, which does not follow the curved *Chandra* focal plane. These curves include the blurs due to the HRC-I spatial resolution and the *Chandra* aspect error.

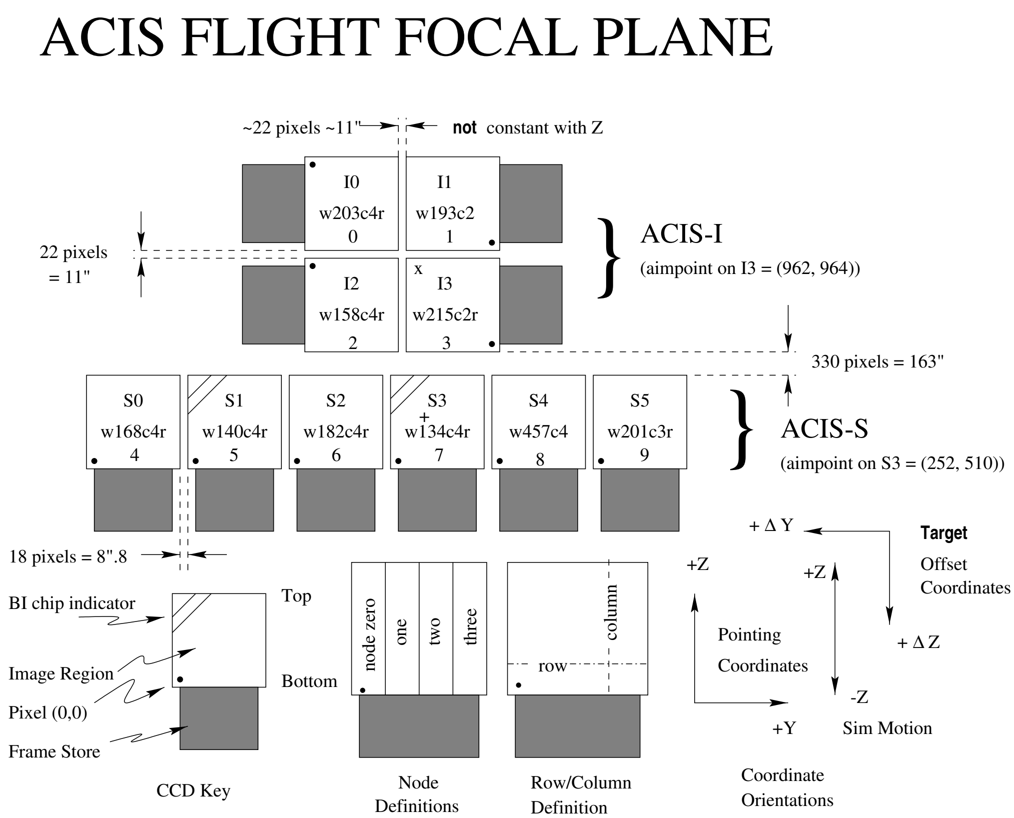

Figure 6.1: A schematic drawing of the ACIS focal plane; insight to the terminology is given in the lower left. Note the nominal aimpoints: on S3 (the '+') and on I3 (the 'x'). On S3, it has become standard practice to add an observatory Y-offset of -20″ (41 pixels) from the true aimpoint (252,510) in the direction of S4 for all ACIS-S observations in order to move the source flux away from the node 0-1 boundary. Note the differences in the orientation of the I and S chips, important when using Subarrays (Section 6.11.3). Note also the (Y, Z) coordinate system and the target offset convention (see Chapter 3) as well as the SIM motion (+/-Z). The view is along the optical axis, from the source toward the detectors, (-X). The numerous ways to refer to a particular CCD are indicated: chip letter+number, chip serial number, and ACIS chip number. The node numbering scheme is illustrated lower center.

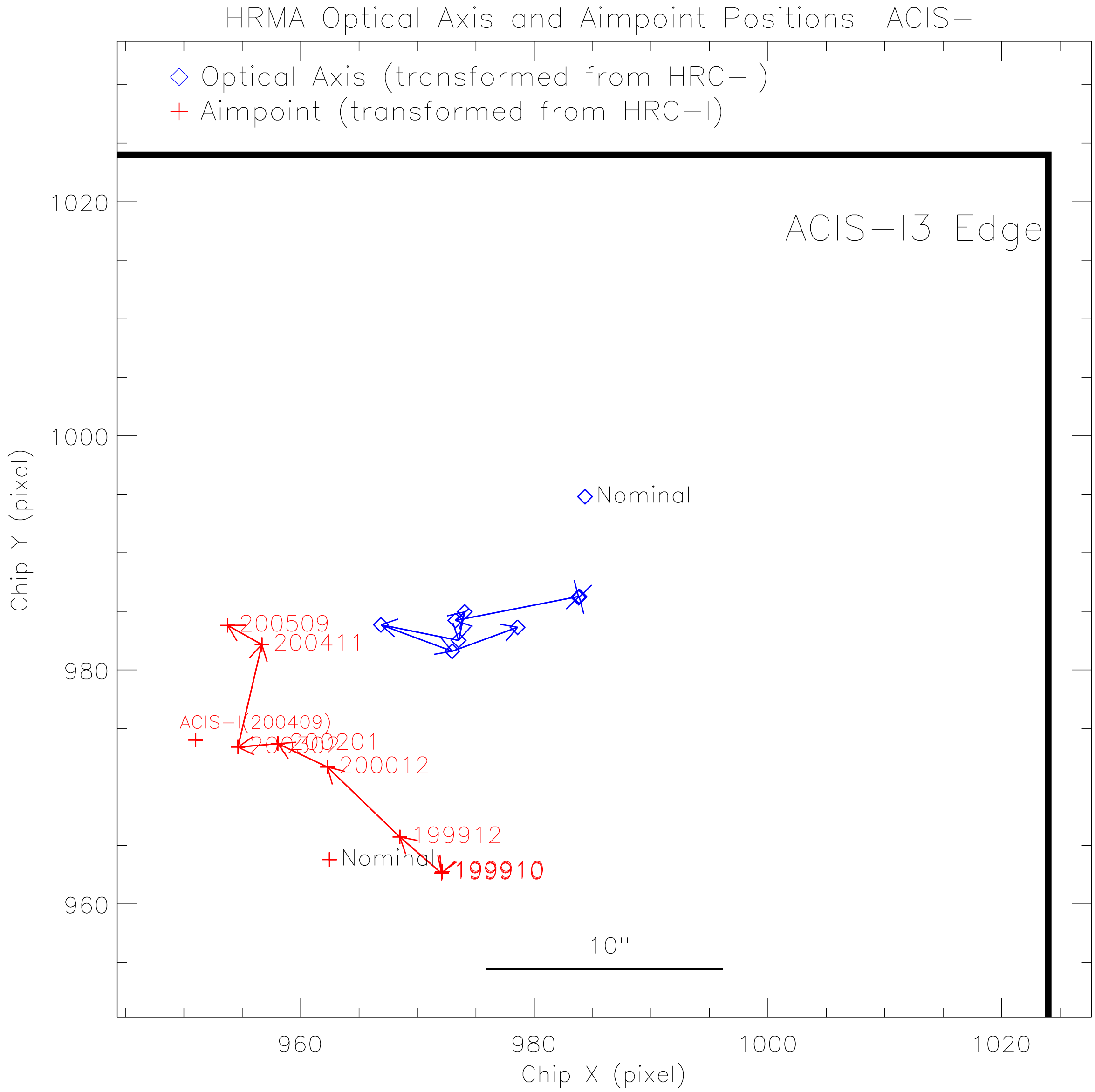

Figure 15: Chandra Optical Axis and Aimpoint positions on ACIS-I, transformed from the HRC-I measurements.

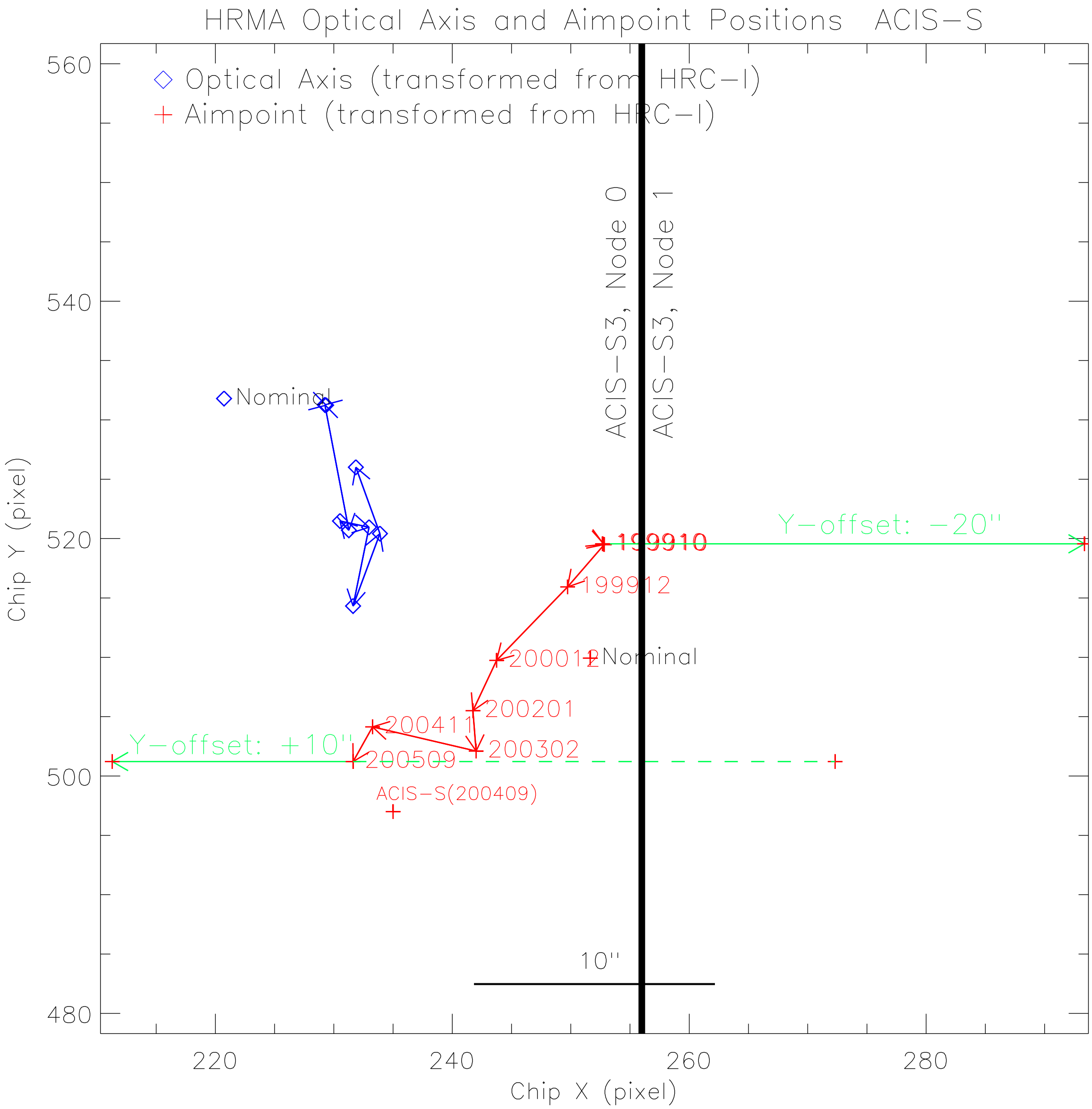

Figure 16: Chandra Optical Axis and Aimpoint positions on ACIS-S, transformed from the HRC-I measurements. Because of the aimpoint drift, the default target pointing offset for ACIS-S observations has been changed from Y-offset=$-20''$ to Y-offset=$+10''$ to avoid the node boundary during dither ($16''$ peak to peak), as announced in Chandra Electronic Bulletin No. 43. This change also puts the target pointing closer to the Optical Axis.